We are IntechOpen,
the world's leading publisher of
Open Access books
Built by scientists, for scientists

6,900
Open access books available

186,000
International authors and editors

200M
Downloads

Our authors are among the

154
Countries delivered to

TOP 1%
most cited scientists

12.2%
Contributors from top 500 universities

BOOK CITATION INDEX
CLARIVATE ANALYTICS
INDEXED

WEB OF SCIENCE™

Selection of our books indexed in the Book Citation Index
in Web of Science™ Core Collection (BKCI)

Interested in publishing with us?
Contact book.department@intechopen.com

Numbers displayed above are based on latest data collected.
For more information visit www.intechopen.com

Flow Evolution Mechanisms of Lid-Driven Cavities

José Rafael Toro and Sergio Pedraza R.
Grupo de Mecánica Computacional, Universidad de Los Andes
Colombia

1. Introduction

The flow in cavities studies the dynamics of motion of a viscous fluid confined within a cavity in which the lower wall has a horizontal motion at constant speed. There exist two important reasons which motivate the study of cavity flows. First is the use of this particular geometry as a benchmark to verify the formulation and implementation of numerical methods and second the study of the dynamics of the flow inside the cavity which become very particular as the Reynolds (Re) number is increased, i.e. decreasing the fluid viscosity.

Most of the studies, concerning flow dynamics inside the cavity, focus their efforts on the steady state, but very few study the mechanisms of evolution or transients until the steady state is achieved (Gustafson, 1991). Own to the latter aproach it was considered interesting to understand the mechanisms associated with the flow evolution until the steady state is reached and the steady state per se, since for different Re numbers (1,000 and 10,000) steady states are "similar" but the transients to reach them are completely different.

In order to study the flow dynamics and the evolution mechanisms to steady state the Lattice Boltzmann Method (LBM) was chosen to solve the dynamic system. The LBM was created in the late 90's as a derivation of the Lattice Gas Automata (LGA). The idea that governs the method is to build simple mesoscale kinetic models that replicate macroscopic physics and after recovering the macro-level (continuum) it obeys the equations that governs it i.e. the Navier Stokes (NS) equations. The motivation for using LBM lies in a computational reason: Is easier to simulate fluid dynamics through a microscopic approach, more general than the continuum approach (Texeira, 1998) and the computational cost is lower than other NS equations solvers. Also is worth to mention that the prime characteristic of the present study and the method itself was that the primitive variables were the vorticity-stream function not as the usual pressure-velocity variables. It was intended, by chosing this approach, to understand in a better way the fluid dynamics because what characterizes the cavity flow is the lower wall movement which creates itself an impulse of vorticiy which is transported within the cavity by diffusion and advection. This transport and the vorticity itself create the different vortex within the cavity and are responsible for its interaction.

In the next sections steady states, periodic flows and feeding mechanisms for different Re numbers are going to be studied within square and deep cavities.

2. Computational domains

The flow within a cavity of height **h** and wide **w** where the bottom wall is moving at constant velocity U_0 Fig.1 is going to be model. The cavity is completely filled by an incompresible fluid with constant density ρ and cinematic viscosity ν.
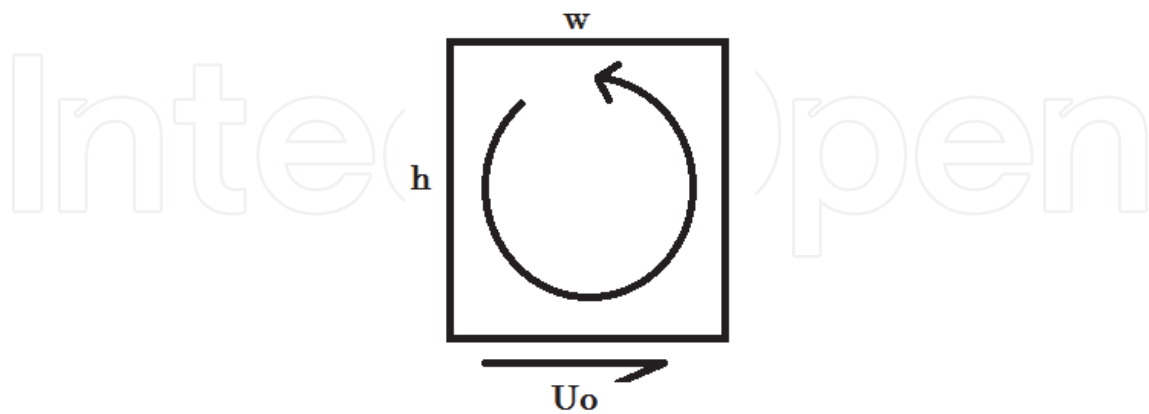

Fig. 1. Cavity

3. Flow modelling by LBM with vorticity stream-function variables

Is important to introduce the equations that govern the vorticity transport and a few definitions that will be used during the present study.

Definition 0.1. *A vortex is a set of fluid particles that moves around a common center*

The vorticity vector is defined as $\omega = \nabla \times v$ and its transport equation is given by

$$\frac{\partial \omega}{\partial t} + [\nabla \omega]v = [\nabla v]\omega + \nu \nabla^2 \omega. \tag{1}$$

which is obtained by calculating the *curl* of the NS equation. For a 2D flow Eq.(1) is simplified to obtain

$$\frac{\partial \omega}{\partial t} + [\nabla \omega]v = \nu \nabla^2 \omega. \tag{2}$$

In order to recover the velocity field from the vorticity field the Poisson equation for the stream function needs to be solved. The Poisson equation wich involves the stream function is stated as

$$\nabla^2 \psi = -\omega \tag{3}$$

where ψ is the stream function who carries the velocity field information as

$$u = \frac{\partial \psi}{\partial y} \ , \ v = -\frac{\partial \psi}{\partial x} \ . \tag{4}$$

and ensures the mass conservation. The motivation for adopting vorticity as the primitive variables lies in the fact that every potential, as the pressure, is eliminated which is physicaly desirable because being the vorticity an angular velocity, the pressure, which is always normal to the fluid can not affect the angular momentum of a fluid element.

3.1 Numerical method

Consider a set of particles that moves in a bidimensional lattice and each particle with a finite number of movements. Now a vorticity distribution function $g_i(x, t)$ will be asigned to each particle with unitary velocity e_i giving to it a dynamic consistent with two principles:

1. Vorticity transport
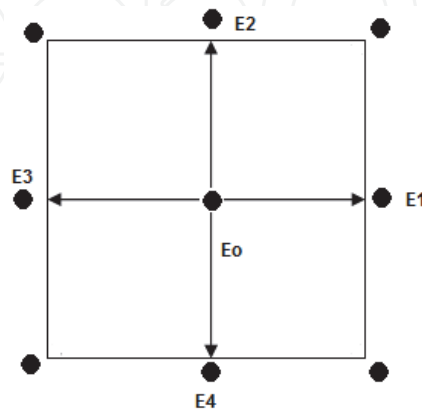
2. Vorticity variation in a node own to particle collision

Fig. 2. D2Q5 Model.2 dimensions and 5 possible directions of moving

Observation 0.2. *The method only considers binary particle collisions.*

The evolution equation is discribed by

$$g_k(\vec{x} + c\vec{e_k}\Delta t, t + \Delta t) - g_k(\vec{x}, t) = -\frac{1}{\tau}[g_k(\vec{x}, t) - g_k^{eq}(\vec{x}, t)]^1 \tag{5}$$

where e_k are the posible directions where the vorticity can be transported as shown in Fig.2. $c = \Delta x/\Delta t$ is the fluid particle speed, Δx and Δt the lattice grid spacing and the time step respectively and τ the dimensionless relaxation time. Clearly Eq.(5) is divided in two parts, the first one emulates the advective term of (1) and the collision term, which is in square brackets, emulates the diffusive term of equation (1).
The equilibrium function is calculed by

$$g_k^{eq} = \frac{w}{5}\left[1 + 2.5\frac{\vec{e_k} \cdot \vec{u}}{c}\right]. \tag{6}$$

The vorticity is calculed as

$$w = \sum_{k \geq 0} g_k \tag{7}$$

and τ, the dimensionless relaxation time, is determined by Re number

$$Re = \frac{5}{2c^2(\tau - 0.5)}. \tag{8}$$

---

[1] The evolution equations were taken from (Chen et al., 2008) and (Chen, 2009). Is strongly recomended to consult the latter references for a deeper understanding of the evolution equations and parameter calculations.

In order to calculate the velocity field Poisson equation must be solved (3). In order to do this (Chen et al., 2008) introduces another evolution equation.

$$f_k(\vec{x} + c\vec{e_k}\Delta t, t + \Delta t) - f_k(\vec{x}, t) = \Omega_k + \hat{\Omega}_k. \tag{9}$$

Where

$$\Omega_k = \frac{-1}{\tau_\psi}[f_k(\vec{x}, t) - f_k^e q(\vec{x}, t)], \quad \hat{\Omega}_k = \Delta t \tilde{\xi}_k \theta D \tag{10}$$

and $D = \frac{c^2}{2}(0.5 - \tau_\psi)$. τ_ψ is the dimensionless relaxation time of the latter evolution equation wich can be chosen arbitrarly. For the sake of understanding the evolution equations, the equation (9) consist on calculating $\frac{D\psi}{Dt} = \nabla^2\psi + \omega$ until $\frac{D\psi}{Dt} = 0$, having found a solution ψ for the Poisson equation.

By last, the equlibrium distribution function is defined as

$$f_k^{eq} = \begin{cases} \zeta_k\psi & k = 1, 2, 3, 4 \\ -\psi & k = 0 \end{cases} \tag{11}$$

where $\tilde{\xi}_k$ and ζ_k are weight parameters of the equation.

3.2 Algorithm implementation

In order to implement the evolution equation Eq.(5) two main calculations are considered. First, the collision term is calculated as

$$g_k^{int} = -\frac{1}{\tau}[g_k(\vec{x}, t) - g_k^{eq}(\vec{x}, t)] \tag{12}$$

and next the vorticity distributions is transported as

$$g_k(\vec{x} + c\vec{e_k}\Delta t, t + \Delta t) = g_k^{int} + g_k(\vec{x}, t) \tag{13}$$

which is, as mentioned, the basic concept that governs the LBM, collisions and transportation of determined distribution in our case a vorticity distibution.

3.2.1 Algorithm and boundary conditions

1. Paramater Inicialization
   - Moving wall velocity: $U_0 = 1$.
   - $\psi|_{\partial\Omega} = 0$, own to the fact that no particle is crossing the walls.
   - $u = v = 0$ in the whole cavity excepting the moving wall.
   - Re number definition[2]

2. Wall vorticity calculation

$$\omega|_{\partial\Omega} = \frac{7\psi_w - 8\psi_{w-1} + \psi_{w-2}}{2\Delta n^2} \tag{14}$$

$$\omega|_{\partial\Omega} = \frac{7\psi_w - 8\psi_{w-1} + \psi_{w-2}}{2\Delta n^2} - \frac{3U_0}{\Delta n} \tag{15}$$

Both equations came from solving Poisson equation Eq.(3) on the walls by a second order Taylor approximation. Eq.(15) is used on the moving wall nodes.

---

[2] For the sake of clarity Re number is imposed in the method by the user which intrinsically is imposing different flow viscosities.

3. Velocity field calculation using Eq.(4)

4. Equilibrium probability calculation using Eq.(6)

5. Colission term calculation using Eq.(12)

6. Probability transport using Eq.(13)

7. Vorticity field calculation using Eq.(7)

8. Solution of Poisson equation: In order to solve Poisson equation the evolution equation Eq.(9) for the stream-function distribution was implemented within a loop wishing to compare f_k's values (i.e. ψ) aiming to achive that $\frac{D\psi}{Dt} = \nabla^2\psi + \omega = 0$. For the latter loop the process terminated when

$$\sum_{x,y} |f_k^+ - f_k| < 10^{-3}.$$

While the simulations were ran, it was found that the algorithm was demanding finer meshes for higher Re numbers, i.e. 700x700 nodes mesh for Re 6,000, increasing the computational cost and most of the times ending in overflows own to the fluid regime. To overcome this situations a turbulence model was introduced to the LBM proposed by (Chen, 2009).

4. Introduction of turbulence in LBM

The principal characteristic of a turbulent flow is that its velocity field is of random nature. Considering this, the velocity field can be split in a deterministic term and in a random term i.e. $U(x,t) = \bar{U}(x,t) + u(x,t)$, being the deterministic and random term respectively. In order to solve the velocity field, the NS equations are recalculated in deterministic variables adding to the set a closure equation own to the loss of information undertaken by solving only the deterministic term. At introducing a turbulent model there exist three different approaches: algebraic models, closure models and Large Eddy Simulations (LES) being the latter used in the present study. LES were introduce by James Deardorff on 1960 (Durbin & Petersson-Rief, 2010). Such simulations are based in the fact that the bulk of the system energy is contained in the large eddys of the flow making not neccesary to calculate all the vortex disipative range which would imply a high computational cost (Durbin & Petersson-Rief, 2010). If small scales are ommited, for example by increasing the spacing by a factor of 5, the number of grid points is substantially reduced by a factor of 125 (Durbin & Petersson-Rief, 2010). In LES context the elimination of these small scales is called filtering. But this filtering or omission of small scales is determined as follows: the dissipative phenomenon is replaced by an alternative that produces correct dissipation levels without requiring small scale simulations. The Smagorinsky model was introduced where another flow viscosity (usually known as subgrid viscosity) is considered which is calculated based on the fluid deformation stress. Specifically it is model as $\nu_t = (C\Delta)^2|S|$Chen et al. (2008) where

$$S_{ij} = \frac{1}{2}\left(\frac{\partial \bar{U}_i}{\partial x_i} + \frac{\partial \bar{U}_j}{\partial x_j}\right),$$

Δ is the filter width and C the Smagorinsky constant. In the present study $C = 0.1$ and $\Delta = \Delta x$. Assuming this new **subgrid viscosity** ν_t the momentum equation is given by

$$\frac{\partial \omega}{\partial t} + [\nabla\omega]v = \frac{\partial}{\partial x}\left(\nu_e \frac{\partial \omega}{\partial x}\right) + \frac{\partial}{\partial y}\left(\nu_e \frac{\partial \omega}{\partial y}\right)$$

where

$$\nu_e = \nu_t + \nu.$$

As the transport equation has changed, the LBM evolution equation has also changed

$$g_k(\vec{x} + c\vec{e_k}\Delta t, t + \Delta t) - g_k(\vec{x}, t) = -\frac{1}{\tau_e}[g_k(\vec{x}, t) - g_k^{eq}(\vec{x}, t)] \qquad (16)$$
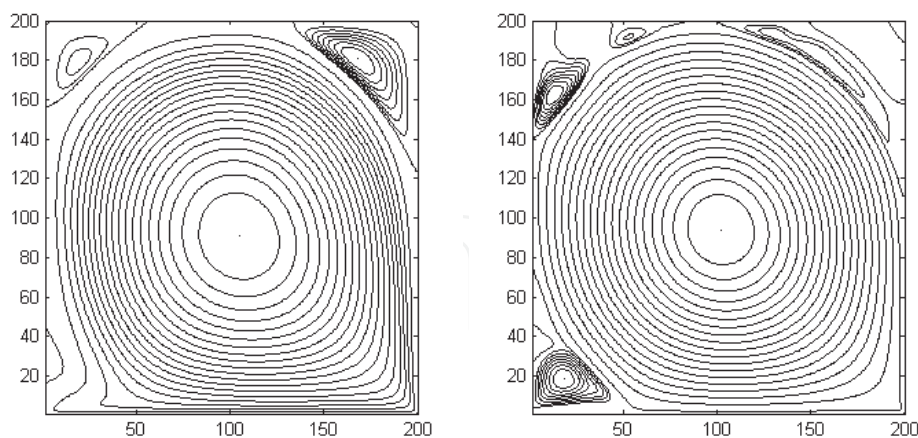
where

$$\tau_e = \tau + \frac{5(C\Delta)^2|S|}{2c^2\Delta t} \quad and \quad |S| = |\omega|^3.$$

Having a new evolution equation Eq.(16) the algorithm has to be modified adding a new step where τ_e is calculated based on the vorticity field. After making this improvement to the method, the algorithm began to work eficiently allowing to achive higher Re numbers without compromising the computer cost, justifing the use of a LBM.

5. Steady state study for different Re numbers

It is said that the flow has reached steady state when collisions and transport do not affect each node probability. Concerning the algorithm it was considered that the flow had reached the steady state when its energy had stabilized and when the maps of vorticity and stream function showed no changes through time.

Steady state vortex configuration for Re 1,000 and Re 10,000 is shown in Fig.3. It worth to notice that both are very similar, a positive vortex that fills the cavity and two negative vortices at the corners of the cavity. This configuration was observed from Re 1,000 to Re 10,000 being a prime characteristic of cavity flows. It is also important to clarify that for Re 10,000 the steady state presents a periodicity which is located in the upper left vortex that we shall see later, indeed Fig.3(b) is a "snapshot" of the flow.

(a) Stream-function map in steady state for Re 1,000. (b) Stream-function map in steady state for Re 10,000.

Fig. 3. Steady states. Maps were taken at 100,000 and 110,000 iterations respectively.

---

[3] Is strongly recomended to consult (Chen, 2009) for a deeper understanding of the evolution equations and parameter calculations.

5.1 Deep cavities

Several studies have proposed to study the deep cavity geometry (Gustafson, 1991; Patil et al., 2006) but none has reached to simulate high Re numbers possibly because the mesh sizes. Due to the LBM low computational cost it was decided to present the study of a deep cavity with an aspect ratio (AR) of 1.5 for Re 8,000.

5.1.1 Vortex dynamics

A general description is presented emphasizing the most important configurations through evolution to steady state:

- **Step 1 Fig.4(a)** The positive vortex creates a negative vortex that arises from the right wall triggering an interaction since the begining of the evolution.

- **Step 2 Fig.4 (b)** The negative vortex that arises from the right wall has taken the whole cavity confining the positive vortex to the bottom.

- **Step 3 Fig.4(c,d)** Positive vortices have joined in one by an interesting process discribed in Sec6. This union creates a "mirror" phenomenon inside the cavity.

- **Step 4 Fig.4(e)** The positive vortex expands into the cavity moving upward the negative vortex until the steady state is reached in which both vortices occupy the same space of the cavity. Is worth to notice that this vortex distribution is not achieved in the square cavity steady state.

5.1.2 Mirror phenomenon

During the evolution it was observed that after positive vortices joined (Fig.4(c, d)) the new big positive vortex acted as a moving wall for the negative vortex injecting vorticity to it. Reproducing the behavior seen in the square cavity, now by the negatie vortex. Ergo a *quasi square cavity* was created in the top of the cavity but instead having a moving wall it had a vortex. The phenomenon is shown in Fig.5 where it is clear that the top of the deep cavity is a "reflection" of the square cavity with respect to an imaginary vertical axis drawn between these two.

6. Vortex binding

A particular process for Re 10,000 in square and deep cavities was found to take place through evolution. This process occurs several times throughout evolution, named Vortex Binding. In this process isolated vortices get connected forming a "massive" vortex which eventually will configure the steady state vortices distribution. A binding process that occured through evolution is shown in Fig.6 binding a positive vortex that appeared in the upper right corner with the positive vortex that came from the movement of the bottom wall.

In order to explain the binding process, which is illustrated in Fig.6, recall the vorticity transport equation Eq.(1). The transport equation is divided in two terms that dictate the transport of vorticity, the diffusive term $\nu\nabla^2\omega$ and the advective term $[\nabla\omega]v$. For a high Re number flow the diffusive term can be neglected, turning the attention in the advective term. As the flow evolved it was seen that the vorticity and stream-function contour lines tended to align as shown in Fig.7(a) making the vorticity gradient vector and velocity vector orthogonal at different places (Fig.7(a)) causing $[\nabla\omega]v = 0$, i.e. no vorticity transport.

As shown in Fig.7(b) vorticity contour lines started to curve, due to its own vorticity, crossing with the stream-function contour lines and making $[\nabla\omega]v \neq 0$. In Fig.7(b)can be seen that
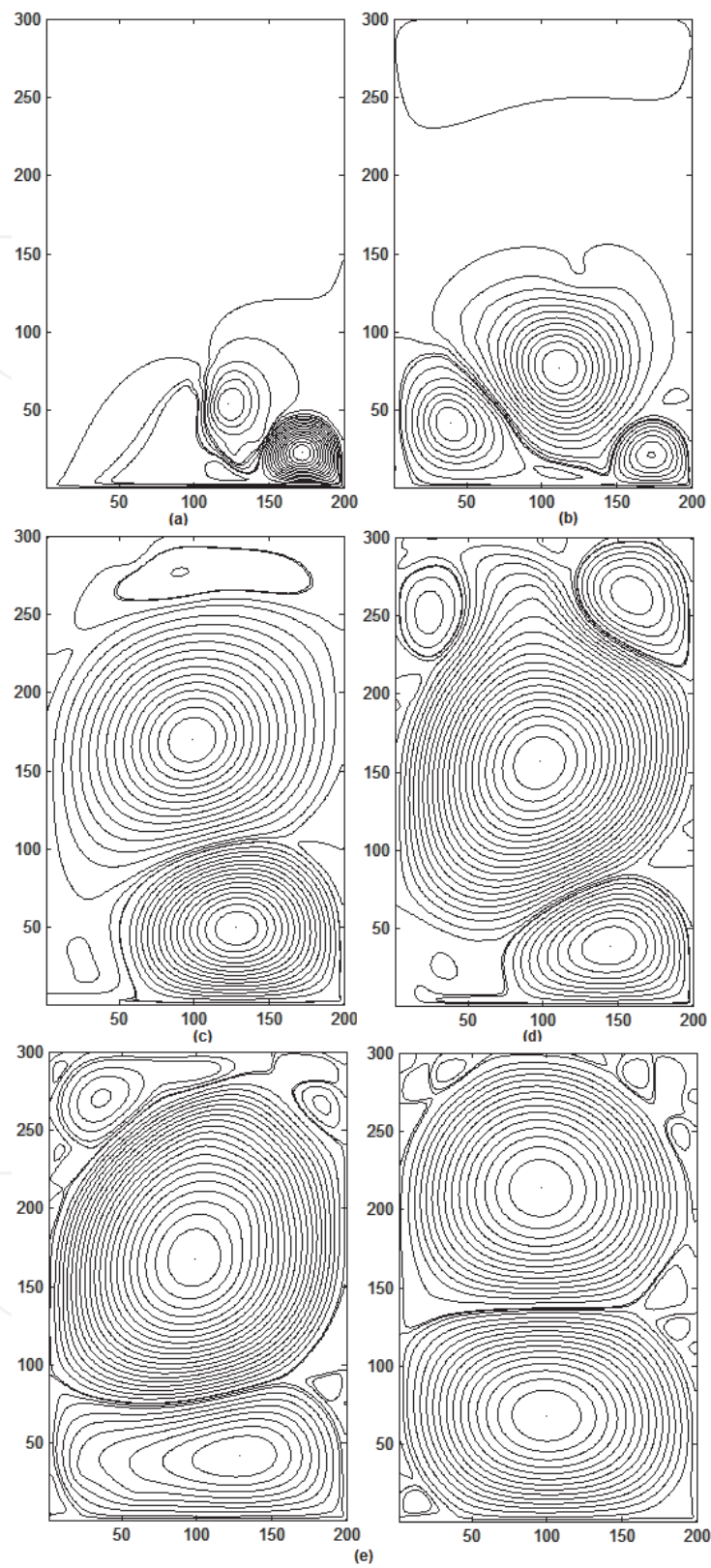
Fig. 4. Stream-function map for different times through evolution for a cavity with AR=1.5 and Re 8,000 in a 200x300 nodes mesh. *a,b,c,d and e* were taken at 20,000, 50,000, 150,000, 180,000 and 260,000-340,000 iterations.
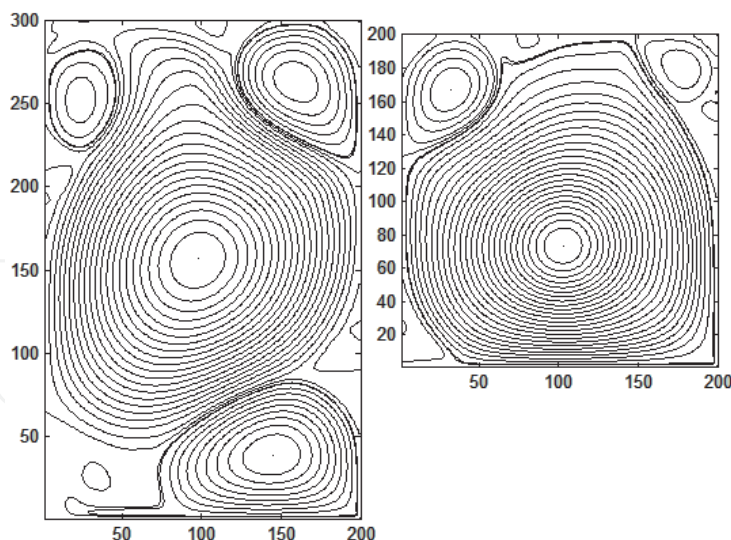
Fig. 5. *Left* Stream-function map for Re 8,000 in a cavity with AR=1.5 (200x300 nodes) *Right* Stream-function map in a square cavity for Re 8,000 (200x200 nodes).
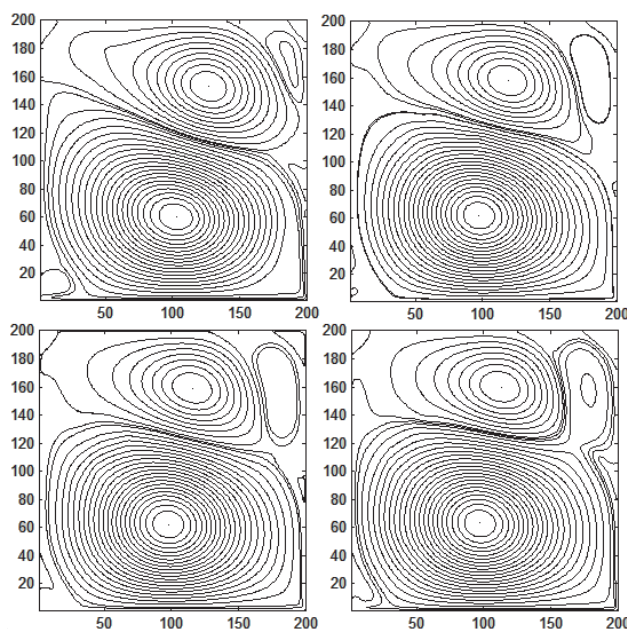

Fig. 6. Stream-function maps for Re 10,000 were Vortex binding process take place. Four maps were taken between 80,000 and 90,000 iterations

the vorticity gradient and the velocity vector are no longer orthogonals creating vorticity transport in different places which made possible the vortex binding to take place.

7. Periodicity in cavity flows

In the study of dynamic systems, being the case of the present study the NS equations, and their solutions there exist bifurcations leading to periodic solutions. Specifically in cavity flows, when the Re number is increased, such bifurcations take place known as **Hopf Bifurcations**. Willing to understand how this Bifurcation takes place the *Sommerfelds* infinitesimal perturbation model is introduced. This perturbation model considers a small

(a) Upper right corner (nodes: 100:200 x 80:200).Taken at 80,000 iterations

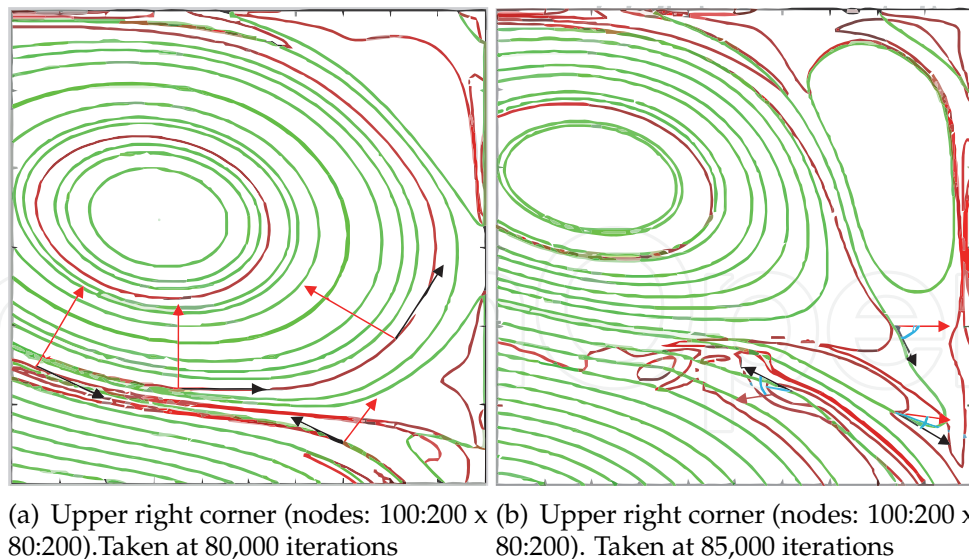(b) Upper right corner (nodes: 100:200 x 80:200). Taken at 85,000 iterations

Fig. 7. *Left* Stream-function contour lines (**Green**), vorticity contour lines(**Red**), vorticity gradient(**Red**), velocity vector(**Black**).*Right* Stream-function contour lines (**Green**), vorticity contour lines(**Red**), vorticity gradient(**Red**), velocity vector(**Black**)and angle between $[\nabla \omega]$ and v(**Blue**)

perturbation of the dynamical system in order to study the equilibrium state or the lack of it. Let be considered the next dynamical system

$$\frac{d\acute{u}}{dt} = [M_\nu]\,\acute{u}. \tag{17}$$

The solution of Eq.(17) lies on finding the eigenvectors of the $[M_\nu]$ operator which is in function of the fluid vicosity. Depending on the Re number the eigenvalues (and eigenvector) can be complex i.e. $\lambda \in \mathbb{C}$, leading to periodic solutions(Toro, 2006) or Bifurcations. In (Auteri et al., 2002) the bifurcation for a cavity flow was located between 8017,6 and 8018,8 (Re numbers) but since 1995 (Goyon, 1995) reported the existence of particular periodic flow located in the upper left corner of a square cavity. In order to find the flow periodicity for Re 10,000 and determine if the system had reached its asymptotic state the system energy was used as a measure. A Periodic flow for a deep cavity is shown in Fig.8[4]

8. Flow transients

Studying vorticity and stream-function maps was found that the way to get to the *same* state in most of the flow (Fig.3(a) and Fig.3(b)), with the exception of the corners for Re 10,000 which oscillate, change significantly as the number of Re varies. In order to illustrate this "bifurcation" vorticity transients for Re 1,000 and Re 10,000 are shown in Figs.9, 10 and 11 until steady state configuration is reached.

8.1 Transient description
For Re 1,000 the positive vortex is created on the lower right corner by the bottom wall movement. Latter vortex is fed and grows until the whole cavity is taken cornering

---

[4] A well discribed periodic flow for square cavity can be found in (Goyon, 1995).

and breaking a negative vortex that has accompanied it since the beginning of evolution without qualitative form changes, only scaling the first configuration until the steady state configuration is achieved in Fig.3(a).
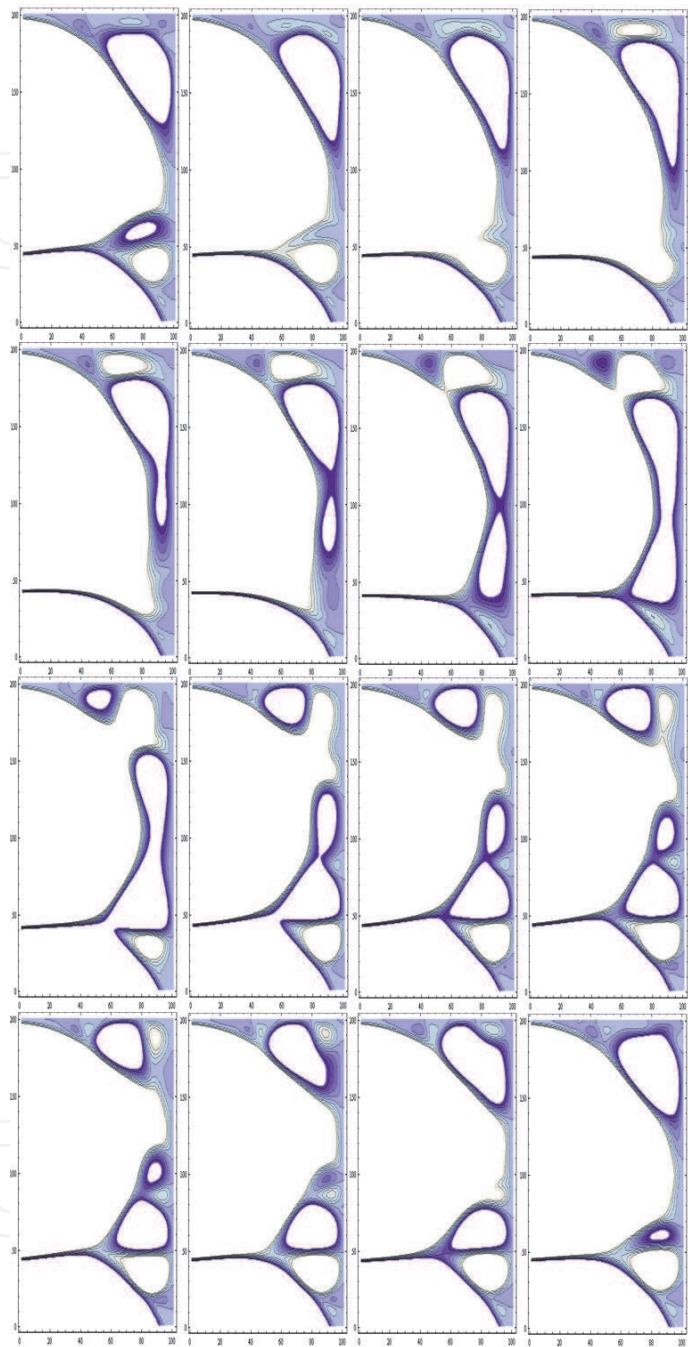

Fig. 8. Stream-function maps for a deep cavity with AR=1.5 and Re 8,000 where periodic flow take place. Maps were taken between 300,000 and 309,000 iterations. *White patches are vortices with high absolute vorticity*. Cavity upper right corner (100:200x100:300) nodes, see Fig.4(e-right)

For Re 10,000 the positive vortex is created due to the lower wall movement and immediately itself creates a negative vortex coming from the right wall. Unlike Re 1,000 these two
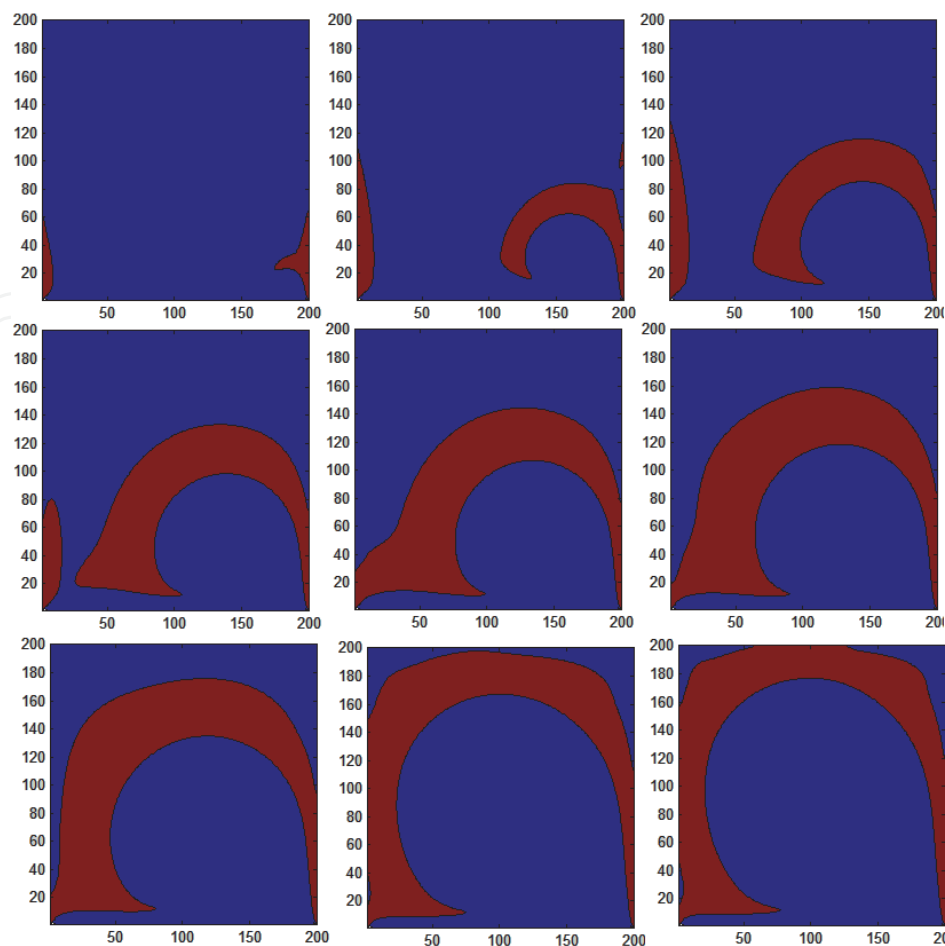
Fig. 9. Vorticity maps: Positive vorticiy (**Blue**), Negative vorticity(**Red**) (200x200 nodes mesh). The nine maps were taken at 10,000, 20,000, 30,000, 40,000, 50,000, 60,000, 70,000, 80,000, 100,000 and 110,000 iterations respectively.

vortices qualitatively change during evolution, changing size and shape until the stable state configuration is reached shown in Fig.3(b).

It is worth to notice that vorticity maps for Re 1,000 and Re 10,000 are topologicaly very different. For Re 1,000 no interaction between positive and negative vorticity is presented but for Re 10,000 interaction is presented since the begining of evolution until the steady state and in the steady state itself because what causes the flow periodicity is the interaction of positive and negative vortices on the corners of the cavity.

9. Vortex feeding mechanisms

Cavity flow is a phenomenon characterized by a continuos vorticity injection to the system induced by the moving wall. The vorticity arises because the no-slip condition (viscous fluid) creating an impulse of vorticity that is transported into the cavity by advection or diffusion Eq.(1). As seen since the beginning the vorticity transport equation is divided in a diffusive term $\nu\nabla^2\omega \approx \frac{1}{Re}\nabla^2\omega$ and in an advective term $[\nabla\omega]\,v$. At the beginning of the flow evolution the vorticity input is transported from the wall purely by diffusion but as the flow evolves both terms of the vorticity transport equation start to have different weights, being the diffusive term the most sensitive to Re number variations.
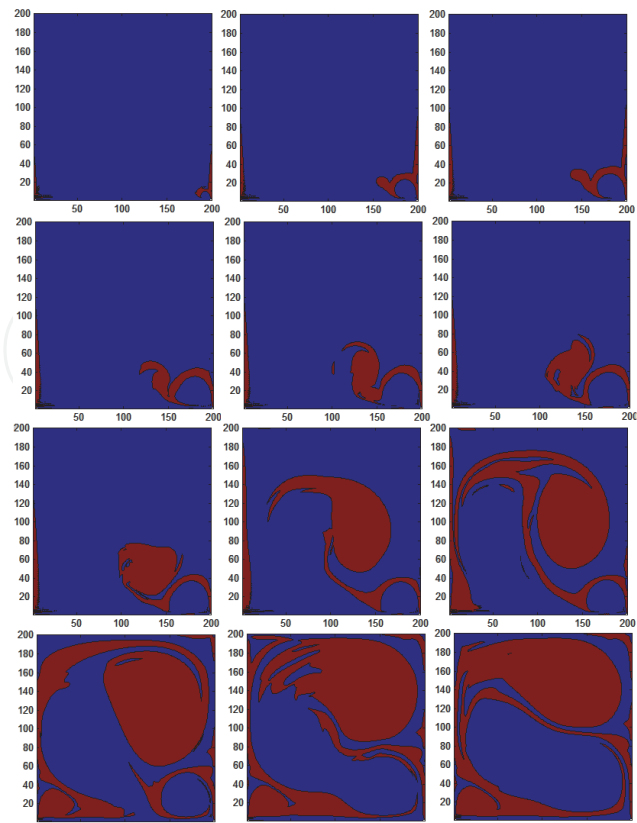
Fig. 10. Vorticity maps: Positive vorticiy (**Blue**), Negative vorticity(**Red**) (200x200 nodes mesh). The twelve maps were taken from 10,000 to 60,000 iterations.
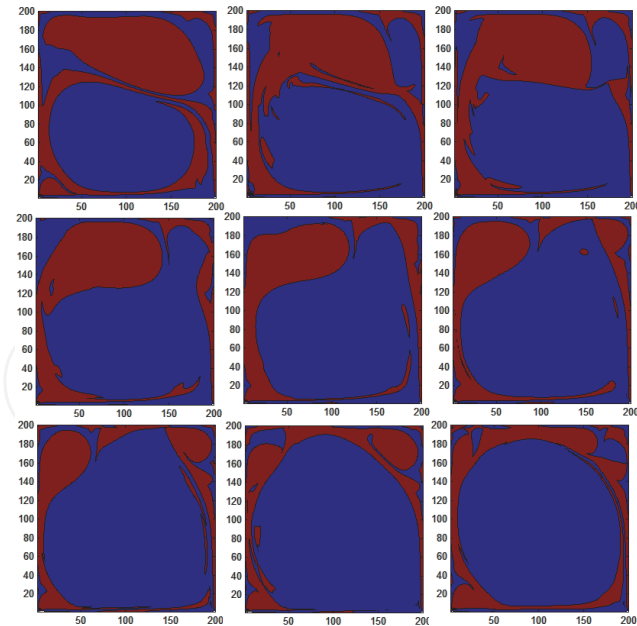

Fig. 11. Vorticity maps: Positive vorticiy (**Blue**), Negative vorticity(**Red**) (200x200 nodes mesh). The nine maps were taken from 60,000 to 110,000 iterations.

Definition 0.3. *A **vorticity channel** is a bondary layer, coming from a wall, that feeds and creates vortex.*

9.1 Channel creation and some other characteristics

Channel creation is derived from two different phenomena: First is the energy transformation that occurs in the wall because the system continually transforms translational energy into rotational energy. Secondly a vortex whatever its sign is creates a channel of opposite sign. In oder to understand the latter suppose a positive vortex near a wall. The vortex make the particles that lie between it and the wall start spinning or *rotate*, due to viscosity, in the opposite direction causing a vorticity input - in this case negative - to the system.

There are three important features on the channels. The first and most important is that the channels transport vorticity from the walls inside the cavity and also diffuses vorticity along the route to nearby channels in proportion to the existing vorticity gradient. Secondly a positive channel always wraps a negative vortex and a negative channel always wraps a positive vortex. And finally channel thickness is function of the Re number.

9.2 Channel study for Re 1,000

- **Channel creation:** The transient is shown in Fig.9. Since the beginning there is a feeding channel from the right wall that grows merging in a left wall channel. It is worth noticing that the channel wraps the positive vortex during evolution (Fig.12(a)) but never interacts with it.

- **Channel characteristics:** In Fig.9 can be observed that the feeding channels are thick. This ows to the fact the diffusive term of the transport equation is big enough to let vorticity be spread within the fluid apart from being transported.

9.3 Channel study for Re 10,000

Before studying the channels it is worth to clarify that in Fig.10 and 11 channels are the thin red "tubes" and the color patches are formed vortices which are fed by channels.

- **Channel creation:** In the transient shown in Fig.10 can be seen since the beginning the appearance of a feeding channel coming from the right wall, but unlike the Re 1,000 transient, it begins to feed a vortex (sixth square of transient Fig.10) that grows inside the cavity. This vortex has the ability to interact in different ways (Fig.10 and 11) with the positive vortex that eventually will take the cavity. What is interesting about the vortex interaction, apart from the different forms that arise in the transient, is that the latter vortex has as many vorticity as the positive one, allowing them to interact in many ways. This interaction is able to produce a configuration seen in the deep cavity steady state where both vortices occupy the cavity without cornering each other but highly unstable (twelfth square Fig.10). This occurs because the diffusive term of the transport equation has less weigh, allowing to concentrate vorticity without being spread across the cavity, which is the case for Re 1,000. It is also important to mention that for Re 10,000 negative channel wraped positive vortex and vice versa (Fig.12(b)) as happens for Re 1,000.

- **Channel characteristics:** Unlike Re 1,000 channels the thickness of Re 10,000 channels are smaller, due to the diffusive low weight term in the vorticity transport equation.

10. Circulation study for different Re numbers

In order to understand more about what is happening with the vorticity of the system was decided to study the circulation behavior. The circulation is defined as $\Gamma = \int \omega dA$. An interesting aspect of the circulation is that, although it must be constant in the system over

(a) Superposition for Re 1,000 during evolution.

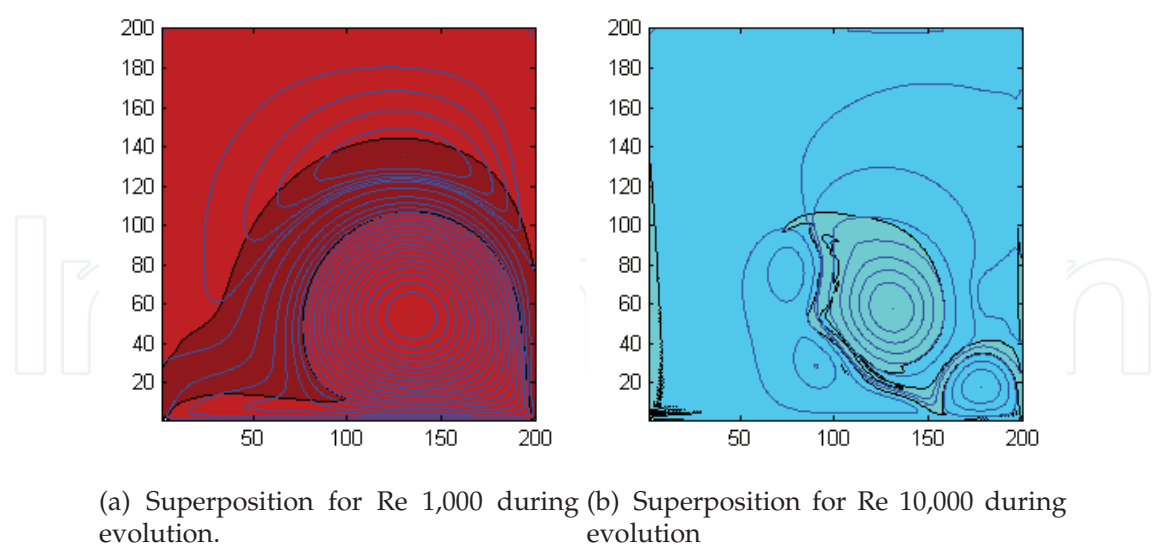(b) Superposition for Re 10,000 during evolution

Fig. 12. Stream-function contour lines (blue) and vorticity maps superposition. *Left* Positive vorticity (Dark red) Negative vorticity (Light red), *right* Positive vorticity (Aqua) Negative vorticity (Aquamarine).

time according to Kelvins theorem, it can be split into positive and negative values. As seen, the prime characteristic of the flow is the positive vorticity input from the lower wall deriving in positve circulation diferential.

(a) Square cavity circulation evolution. Positive Γ (Red) and negative Γ (Blue)

(b) Square cavity circulation evolution. Positive Γ (Red) and negative Γ (Blue)

Fig. 13. *Left* Square cavity circulation for Re 1,000. *Right* Square cavity circulation for Re 10,000.

In both figures can be seen that the flow reaches a maximum around the 100.000 iterations when the positive vortex has taken all the cavity (Fig.3.1 and 3.2). What is interesting are the values of circulation that are achieved for each value of Re (Table.1).

Several important things are shown in Table.1. First the circulation increase for Re 10,000 is three times bigger than Re 1,000 i.e. $\Delta\Gamma_{Re1,000} = 18.36$ compared with $\Delta\Gamma_{Re10,000} = 50.5$. Latter observation means that as the viscosity decreases the system is able to accumulate more circulation. Finally, system circulation is consistent whit Kelvin's theorem even though

	Re 1,000		Re 10,000	
	max	min	max	min
Positive Γ	48.52	30.16	83.5	33
Negative Γ	23.8	3.09	60.67	2.55

Table 1. Circulation values comparison

positive circulation increases negative circulation increases too maintaining a circulation differential of about 30 throughout evolution (Fig.13 a and b).

10.1 Why does the circulation fall after rising for Re 10,000?

It can be seen in Fig.13 that for Re 1,000 positive (negative) circulation reaches its maximum (minimum) and stabilizes around latter value, which fails to happen for Re 10,000 where circulation peaks at a "constant" rate but after reaching maximum starts decreasing. The motivation of this subsection is to explain why this change of slope took place (Fig.13(b)) and try to predict it analiticaly because it was observed that for different Re numbers the same change in slope occures reaching different values of maximum circulation.

In order to understand this phenomena recall that the cavity has vorticity channels that feed and remove vorticity into and out the system affecting the circulation values. Having mentioned this observation and due to the low weight diffusive term has in the transport equation, $\frac{d\Gamma}{dt}$ is calculed according to the gradient of vorticity on the walls (18), which is the same as quantifying how much vorticity is entering and leaving the system.

$$\frac{d\Gamma}{dt} = \int_{\partial\Omega} \nabla w \cdot n ds \tag{18}$$

After ploting Eq.(18) through time it was found that $\frac{d\Gamma}{dt}$ was constant until 100.000 iterations, which is when the positive vortex has taken the cavity, reflecting the "constant" increase of circulation Fig.13(b). More interesting and contradicting the assumption made was that $\frac{d\Gamma}{dt}$ does not fall after the 100,000 iterations, situation that was expected since a slope change was observed in the Fig.13(b) after 100,000 iterations. Willing to explain this behavior the following hypothesis was proposed:

Assume a unit of vorticity entering to the system Fig.14.

This unit feeds the positive vortex. The vortex is not able to accumulate more circulation, as it has reached the steady state configuration therefore this unit of vorticty has to be "passed" to each of the corner vortices, which also are not able to accumulate more circulation having to pass it to the upper wall and balancing the accounts of vorticity on the walls. Since the way of calculating the $\frac{d\Gamma}{dt}$ is based on counting how much vorticity is entering and leaving the system the circulation loss between vortice was not quantified, explaining why $\frac{d\Gamma}{dt}$ remains constant.

11. Discussion and open questions

Through the present study was seen that viscosity is who decides if vorticity can travel without diffusing itself, curl up, accumulate and form vortices. In a word is who decides how will the flow evolves. The interesting thing is that after being so influential in the flow pattern everything was in vain because the configuration of steady state regardless of the number Re (100-10,000) is very similar, a positive vortex has taken the cavity and two or three vortices were cornered. Latter observation trigger on of the most important remaining open
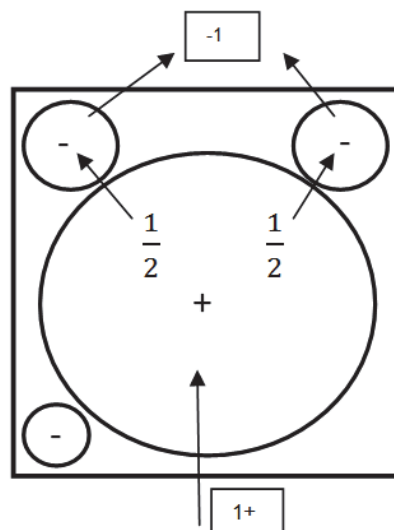
Fig. 14. Vortex diagram

question for future studies, why after so many turns, so many games, the flow reaches the same configuration?. It is believed that a study from game theory involving two players, "positive vorticity" and "negative vorticity" who fight a common good, the space of the cavity, can clarify why the positive vortex end taking the whole cavity behavior that is not achieved in the deep cavity scenario. Along with the latter question, other two remain open. First would be to answer, why the configuration of stable state coincide when the system can not store more vorticity and secondly why can not be achieved by the square cavit flow the configuration that occurs to happen in the deep cavity between the positive and negative knowing before that during the flow evolution this configuration is achieved but then lost.

12. Conclusions

Among all the results it was clearly seen the power and the preponderance of the viscosity in the evolution of cavity flows, how it affects the dynamics of vortices, transient or evolution of the flow and the accumulation or dissipation of energy. Was also observed the periodicity of steady-state flow for both cavities being the first to show a complete cycle of periodicity in the deep one. In conjunction with the above the feeding channels definition were proposed which were key to understanding the transient flow. It was also proposed a transient "Bifurcation" since they vary dramatically as the number of Re is increased. This "Bifurcation" is mainly due to viscosity.
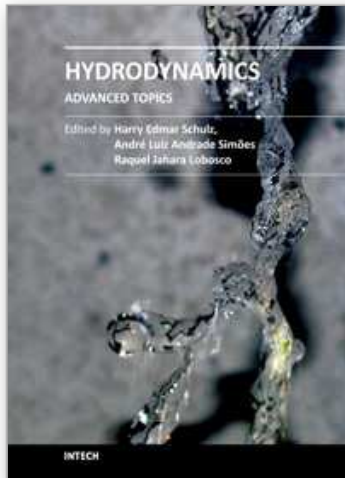
As for deep cavities in addition to finding the periodicity of the flow for Re 8.000 it was presented an interesting phenomenon observed in Sec.5.1.2 where a *quasi cavity* is created that replicates cavity flow transients that occur before reaching steady state in a square cavity. Finally, the numerical method implemented, based on the equations presented in (Chen, 2009; Chen et al., 2008), was a great help for the simplicity of its programming and its primitive variable, vorticity, was central in the study.

13. Acknowledgments

14. References

Auteri, F., Parolini, N. & Quartapelle, L. (2002). Numerical investigation on the stabilityof singular driven cavity flow, *Journal of Computational Physics* 183: 1–25.

Chen, S. (2009). A large-eddy-bassed lattice boltzmann model for turbulent flow simulation, *Applied mathematics and computation* .

Chen, S. & Doolen, G. (1998). Lattice boltzmann method for fluid flows, *Annu. Rev. Fluid Mech.* pp. 329–364.

Chen, S., Toelke, J. & Krafczyk, M. (2008). A new method for the numerical solution of vorticity-Űstreamfunction formulations, *Computational methods Appl. Mech. Engrg.* (198): 367–376.

Durbin, P. & Petersson-Rief, B. (2010). *Statistical theory and modeling for turbulent flow*, Wiley, UK.

Goyon, O. (1995). High-reynolds number solutions of navier-stokes equations using incremental unknowns, *Computer Methods in Applied Mechanics and Engineering* 130: 319–335.

Gustafson, K. E. (1991). Four principles of vortex motion, *Society for Industrial and Applied Mathematics* pp. 95–141.

Hou, S., Q.Zou & S.Chen (1995). Simulation of cavity flow by the lattice boltzmann method, *Computational Physics* (118): 329–347.

Patil, D., Lakshmisha, K. & Rogg, B. (2006). Lattice boltzmann simulation of lid-driven flow in deep cavities, *Computers and Fluids* 35: 1116–1125.

Pope, S. (2000). *Turbulent Flows*, second edn, Cambridge Unversity Press, Cambridge U.K.

Texeira, C. (1998). Incorporation turbulence model into the lattice boltzmann method, *Internationa Journal of modern Physics* (8): 1159–1175.

Toro, J. (2006). *Dinámica de fluidos con introducción a la teoría de turbulencia*, Publicaciones Uniandes, Bogotá.

Hydrodynamics - Advanced Topics

Edited by Prof. Harry Schulz

The phenomena related to the flow of fluids are generally complex, and difficult to quantify. New approaches - considering points of view still not explored - may introduce useful tools in the study of Hydrodynamics and the related transport phenomena. The details of the flows and the properties of the fluids must be considered on a very small scale perspective. Consequently, new concepts and tools are generated to better describe the fluids and their properties. This volume presents conclusions about advanced topics of calculated and observed flows. It contains eighteen chapters, organized in five sections: 1) Mathematical Models in Fluid Mechanics, 2) Biological Applications and Biohydrodynamics, 3) Detailed Experimental Analyses of Fluids and Flows, 4) Radiation-, Electro-, Magnetohydrodynamics, and Magnetorheology, 5) Special Topics on Simulations and Experimental Data. These chapters present new points of view about methods and tools used in Hydrodynamics.

How to reference

In order to correctly reference this scholarly work, feel free to copy and paste the following:

INTECH
open science | open minds